Published in final edited form as:
Dalton Trans. 2012 March 7; 41(9): 2764–2773. doi:10.1039/c2dt12083f.

Ruthenium(II) arene complexes with chelating chloroquine analogue ligands: Synthesis, characterization and *in vitro* antimalarial activity†

Lotta Glans[a], **Andreas Ehnbom**[a], **Carmen de Kock**[b], **Alberto Martínez**[c], **Jesús Estrada**[c], **Peter J. Smith**[b], **Matti Haukka**[d], **Roberto A. Sánchez-Delgado**[c,*], and **Ebbe Nordlander**[a,*]

[a]Inorganic Chemistry Research Group, Chemical Physics, Center for Chemistry and Chemical Engineering, Lund University, Box 124, SE-221 00 Lund, Sweden [2]Division of Pharmacology, Department of Medicine, University of Cape Town Medical School, Observatory 7925, South Africa [c]Department of Chemistry, Brooklyn College and The Graduate Center, The City University of New York, CUNY, 2900 Bedford Avenue, Brooklyn, New York 11210, U.S.A [d]Department of Chemistry, University of Eastern Finland, Box 111, FIN-80101 Joensuu, Finland

Abstract

Three new ruthenium complexes with bidentate chloroquine analogue ligands, [Ru(η^6-cym)($\mathbf{L^1}$)Cl]Cl (**1**, cym = *p*-cymene, $\mathbf{L^1}$ = *N*-(2-((pyridin-2-yl)methylamino)ethyl)-7-chloroquinolin-4-amine), [Ru(η^6-cym)($\mathbf{L^2}$)Cl]Cl (**2**, $\mathbf{L^2}$ = *N*-(2-((1-methyl-1H-imidazol-2-yl)methylamino)ethyl)-7-chloroquinolin-4-amine) and [Ru(η^6-cym)($\mathbf{L^3}$)Cl] (**3**, $\mathbf{L^3}$ = *N*-(2-((2-hydroxyphenyl)methylimino)ethyl)-7-chloroquinolin-4-amine) have been synthesized and characterized. In addition, the X-ray crystal structure of **2** is reported. The antimalarial activity of complexes **1–3** and ligands $\mathbf{L^1}$, $\mathbf{L^2}$ and $\mathbf{L^3}$, as well as the compound *N*-(2-(bis((pyridin-2-yl)methyl)amino)ethyl)-7-chloroquinolin-4-amine ($\mathbf{L^4}$), against chloroquine sensitive and chloroquine resistant *Plasmodium falciparum* malaria strains was evaluated. While **1** and **2** are less active than the corresponding ligands, **3** exhibits high antimalarial activity. The chloroquine analogue $\mathbf{L^2}$ also shows good activity against both the choloroquine sensitive and the chloroquine resistant strains. Heme aggregation inhibition activity (HAIA) at an aqueous buffer/n-octanol interface ($HAIR_{50}$) and lipophilicity (D, as measured by water/n-octanol distribution coefficients) have been measured for all ligands and metal complexes. A direct correlation between the D and $HAIR_{50}$ properties cannot be made because of the relative structural diversity of the complexes, but it may be noted that these properties are enhanced upon complexation of the *inactive* ligand $\mathbf{L^3}$ to ruthenium, to give a metal complex (**3**) with promising antimalarial activity.

Introduction

Malaria has been afflicting mankind for 500 000 years, and in the 21st century the disease remains as lethal as ever.[1] Recent reports by WHO estimate 234 million cases and 860 000 deaths in 2008, numbers that are representative for recent years.[2] Although there is cause for optimism within some areas of the battle against malaria - especially as the funding available for malaria control has increased dramatically - serious obstacles remain, *e.g*. the resistance to common antimalarial drugs. The question of resistance is now more current than ever, after reports of resistance to artemisinins,[3,4] drugs that are part of the

†Electronic Supplementary Information available:

*Corresponding author: Ebbe.Nordlander@chemphys.lu.se; Tel: +46 46 222 8118; Fax: +46 46 222 4119.

recommended first line treatment for infection by the most lethal of the malaria parasites, *Plasmodium falciparum*.[2]

Chloroquine (CQ, Fig. 1) is one of the most successful antimalarial drugs and was for decades the primary chemotherapy used to treat malaria.[5] In its erythrocytic phase, the malaria parasite digests red blood cells, releasing lethal free heme. In the acidic food vacuole of the parasite, heme is detoxified through a biomineralization process which converts it into a non-toxic crystalline dimer known as hemozoin.[6] The commonly accepted mechanism of action of chloroquine and related 4-aminoquinoline drugs involves binding hematin and inhibiting its conversion into hemozoin.[6–11] It has been shown that the 7-chloro-4-aminoquinoline nucleus of chloroquine is responsible for inhibition of hemozoin formation, while the basic quinoline nitrogen and the amine side chain assist accumulation of the molecule in the food vacuole.[12,13]

Widespread resistance has rendered chloroquine useless in most malaria-endemic countries, but it is still the recommended treatment for *Plasmodium vivax* malarial cases in parts of the world.[2,14] Although the mechanism of resistance to chloroquine is not yet fully understood, it seems to be related to mutations in the *Plasmodium falciparum* chloroquine resistance transporter (PfCRT) transmembrane protein, located at the membrane of the digestive vacuole of the parasite.[13,15–18] The mutated protein is able to recognize and expel chloroquine from the food vacuole by mechanisms that are still subject to debate[19] and that **results** in a dramatic decrease of drug concentration at the active site. Therefore new antimalarial drugs capable of overcoming resistance are urgently needed. The ability of the PfCRT protein to extrude chloroquine from the digestive vacuole strongly depends on the lipophilicity of the drug as well as on its structural features.[18,20,21] In addition, there is clear evidence indicating that the formation of hemozoin crystals occurs at water/lipid interfaces.[22–24] Thus, the design of new antiplasmodial agents aimed at CQ-resistant parasites must take into consideration not only their heme aggregation inhibition activity (HAIA) but also structural and physicochemical factors.

Numerous chloroquine analogues have been synthesized during the last decades; one of the most original, and potentially most successful, being the organometallic derivative ferroquine (Fig. 1).[25] Ferroquine exhibits a completely restored activity against resistant parasite strains and has entered phase IIb clinical trials in association with artesunate.[25–28] Other reported organometallic and inorganic derivatives of chloroquine include ruthenocene compounds and half sandwich compounds of chromium and rhenium, as well as ruthenium, rhodium and gold coordination complexes.[29–35]

Ruthenium arene half sandwich complexes have recently received increasing attention as prospective metal-based anticancer drugs and a number of complexes, mostly with nitrogen and phosphorus ligands, are being investigated for their drug candidate potential.[36–39] Combining the versatility of ruthenium arene compounds with the interesting properties of metal-chloroquine derivates, a family of ruthenium half sandwich compounds with chloroquine as ligand was recently reported (Fig. 1). These compounds showed an increased antimalarial activity against chloroquine resistant parasite strains compared to free chloroquine, as well as anticancer properties against several tumour cell lines.[40] A detailed study of factors relating to the antimalarial mechanism of action of these complexes indicated that the increased activity was likely to originate primarily in the major change in lipophilicity and structure of the Ru complexes as compared to chloroquine itself (see Results and Discussion).[41] However, the coordination of chloroquine in these complexes occurred through the quinoline nitrogen (Fig. 1), which has been shown to be crucial for the antimalarial activity.[12] Here we report the synthesis and characterization of a new group of ruthenium arene complexes containing chloroquine analogue ligands with N,N- or Schiff

base N,O-donor moieties, and an investigation of the antimalarial activity of the ruthenium complexes as well as the ligands. We also report some relevant physicochemical studies of their lipophilicity and heme aggregation inhibition ability in an attempt to better account for the observed biological properties.

Results and discussion

Synthesis and characterization

Ligands **L^1–L^4** (Fig. 2) were synthesized following standard synthetic protocols (*cf.* Experimental section). To synthesize *N*-(2-((pyridin-2-yl)methylamino)ethyl)-7-chloroquinolin-4-amine (**L^1**), *N*-(2-aminoethyl)-7-chloroquinolin-4-amine and 2-pyridine carboxaldehyde were stirred overnight at room temperature to form the imine, which was in turn reduced with sodium borohydride to give the desired product in good yield. However, when this reaction was carried out with 3 equivalents of aldehyde and sodium tris(acetoxy)borohydride as reducing agent, the disubstituted ligand *N*-(2-(bis((pyridin-2-yl)methyl)amino)ethyl)-7-chloroquinolin-4-amine (**L^4**) was formed. The ligand *N*-(2-((1-methyl-1H-imidazol-2-yl)methylamino)ethyl)-7-chloroquinolin-4-amine (**L^2**)was synthesized analogously to **L^1**. In contrast, *N*-(2-((2-hydroxyphenyl)methylimino)ethyl)-7-chloroquinolin-4-amine (**L^3**) was isolated in the imine form, after stirring the starting materials together in ethanol at room temperature. Reaction of ligands **L^1** or **L^2** with the [(*p*-cymene)$RuCl_2$]$_2$ dimer in 2:1 molar ratio in dichloromethane at room temperature gave the complexes [RuCl(*p*-cymene)(L)]Cl(L = **L^1**(**1**); **L^2** (**2**)) in good yields (Scheme 1). For ligand **L^3**, deprotonation by triethylamine followed by stirring with the ruthenium *p*-cymene dimer gave the complex [RuCl(*p*-cymene)(**L^3**)] (**3**). All complexes were isolated as yellow or orange air-stable solids with good solubility in polar solvents.

The structure of **2** could be confirmed by single crystal X-ray diffraction (Fig. 3, *vide infra*). The NMR and mass spectra of **1** and **3** strongly support that the structures of these complexes are analogous to that of **2**. The mass spectra of complexes **1–3** show fragmentation patterns that are in agreement with bidentate coordination of ligands **L^1–L^3** (see ESI), and half sandwich (η^6-arene)Ru complexes of ligands based on a picolylamine motif that coordinates in a bidentate fashion to the ruthenium atom are previously known.[42–44] Similarly, there are previous examples of complexes analogous to **3**, with the ligand coordinating to ruthenium through the imine nitrogen and the hydroxyl oxygen.[45–47]

NMR spectroscopy

Unsymmetrical N,N- and N,O-donor ligands induce chirality at the metal atom upon coordination to the (η^6-*p*-cymene)Ru fragment, resulting in loss of two-fold symmetry of the *p*-cymene moiety. Hence, in the ^{1}H NMR spectra of **1–3** the aromatic protons of the *p*-cymene are observed as four separate doublets and the isopropyl group as two doublets, one for each methyl group. For **1** and **2**, the methylene protons adjacent to the coordinated amine show diastereotopic splitting, consistent with a bidentate coordination mode. In the ^{1}H NMR spectrum of **1** in $CDCl_3$, one set of peaks was present, but upon dissolution of **1** in DMSO-d_6 two sets of signals of different relative intensities were observed. The less intense signal set increased with time until equilibrium was reached, after which the distribution of species remained stable; this is demonstrated in Figure 4, which shows the emergence of the second set of signals for the H5 proton of the pyridine moiety over time. A similar behaviour was observed in CD_3OD. The solution behaviour of **2** differed slightly from that of **1**, as the emergence of the second set of signals in the ^{1}H NMR spectrum was slower. Five days after dissolution in DMSO-d_6, the relationship between the two species was 1:0.17 for **2**, while for **1** a 1:1 relationship was reached within 24 h. It is possible that this difference may be related to the larger ring strain of the imidazole relative to the pyridine. In both cases, both

sets of signals differed from those of the free ligand, so decomplexation was ruled out as a possible explanation for the observed equilibrium. Complex **3** displayed only one set of signals in DMSO-d_6, as well as in $CDCl_3$. The most likely explanation for the observed solution behaviour of **1** and **2** is the exchange of the coordinated chloride for a molecule of solvent (DMSO, MeOH, *vide infra*). The alternative explanation that the two observed species correspond to two diastereomers may be ruled out since only one species is observed in $CDCl_3$.

Conductivity measurements

In order to gain further knowledge of the behaviour of the new complexes in solution and better interpret the NMR spectroscopy results, their electrical conductance was measured. Molar conductivity values of 279 and 293 $ohm^{-1}cm^2mol^{-1}$ for 1 mM aqueous solutions of **1** and **2**, respectively, are within the normal range for three ions and indicate that these two complexes undergo rapid hydrolysis to form [Ru(*p*-cymene)(ligand)(H_2O)][Cl]$_2$; these conductivity values remain essentially unchanged after 3 h (299 and 306 $ohm^{-1}cm^2mol^{-1}$ for **1** and **2**, respectively). For complex **3**, a conductivity value of 249 $ohm^{-1}cm^2mol^{-1}$ (or 266 $ohm^{-1}cm^2mol^{-1}$ after 3 h) also indicates the presence of three ions in solution, rather than the two expected for aquation of the complex to yield [Ru(*p*-cymene)(**L**^{3})(H_2O)][Cl]; a possible explanation for this unusual value is that the phenoxy group of the ligand is detached in solution and replaced by a second water molecule. The ^{1}H NMR spectrum of **3** in D_2O shows that the ligand is no longer bidentate, as the *p*-cymene peak pattern is that of a symmetric complex (i.e. two doublets for the aromatic protons). Signals for the coordinated ligand of 1:1 intensity to the *p*-cymene are also observed.

More interesting, the molar conductivity values of 1 mM solutions of the various complexes in DMSO, the solvent in which two sets of NMR signals were observed (and which was used in biological experiments, see Experimental section), are 48.3 $ohm^{-1}cm^2mol^{-1}$ for **1** and 52.1 $ohm^{-1}cm^2mol^{-1}$ for **2**, respectively. These values are intermediate between those corresponding to two and three ions,[48,49] which indicates partial displacement of the coordinated chloride by DMSO to produce equilibrium mixtures of [RuCl(*p*-cymene)(ligand)][Cl] and [Ru(*p*-cymene)(ligand)(DMSO)][Cl]$_2$ (Eq. 1). Such equilibria are fully consistent with the two independent sets of signals appearing in the NMR spectra of **1** and **2**. On the other hand, the conductivity of **3** (33.8 $ohm^{-1}cm^2mol^{-1}$) corresponds to two ions in solution, most likely resulting from full displacement of the chloride to yield exclusively [Ru(*p*-cymene)(**L**^{3})(DMSO)]Cl (Eq. 1).

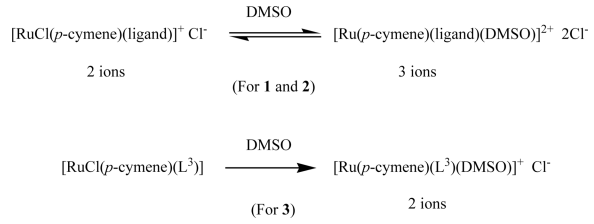

Eq.1

X-ray crystallography

The ruthenium complex **2** was characterised by X-ray crystallography. Suitable crystals were grown from acetone at −20 °C. The molecular structure of **2** is shown in Fig. 3 and relevant crystallographic data are summarized in Table 1. To our knowledge, this crystal structure is unique in being the first half sandwich complex with a pendant 4-amino-7-chloroquinoline moiety; the only previously reported structures are of metallocene

aminoquinoline conjugates.[30] The complex crystallizes as a racemate, and each molecule possesses the expected piano stool geometry, with the two nitrogens of the imidazole and neighbouring amine and the chloro ligand as the legs of the stool. The counter ion Cl^- (omitted in Fig. 3) is engaged in hydrogen bonding with the two NH groups framing the ethylene spacer (cf. ESI). There are very few examples of piano stool ruthenium arene complexes with a bidentate imidazole ligand,[50,51] but the molecular structure of **2** closely resembles corresponding picolylamine complexes with respect to the immediate coordination environment of the metal.[42,43,45] As is expected in this class of structures, the arene ring of the coordinated *p*-cymene is essentially planar, with the distance between the ruthenium atom and the *p*-cymene ring centroid being 1.66 Å and Ru-C_{arene} bonds ranging between 2.165(2) and 2.213(2) Å. This agrees well with similar complexes.[43,52,53] The Ru-Cl, Ru-N_{amine} and Ru-$N_{imidazole}$ bonds (2.422(3), 2.169(1) and 2.078(1) Å, respectively) are also similar to distances reported for related complexes. The Ru-N_{amine} bond is longer than the Ru-$N_{imidazole}$ bond, a pattern that mirrors corresponding picolylamine structures.[42,43,45]

Antimalarial activity and cytotoxicity towards normal mammalian cells

To our knowledge, the antimalarial activities of ligands $\mathbf{L^1}$–$\mathbf{L^4}$ have not been reported previously.[54] Therefore, the antimalarial activities of complexes **1–3** as well as of ligands $\mathbf{L^1}$–$\mathbf{L^4}$ were evaluated *in vitro* against chloroquine sensitive (D10) and chloroquine resistant (Dd2) *Plasmodium falciparum* strains (Table 2). Ligand $\mathbf{L^4}$ was included in the antimalarial study as a comparison to $\mathbf{L^1}$, even though a corresponding metal complex had not been synthesized. The standard drug chloroquine diphosphate was used as reference in all assays. Ligands $\mathbf{L^1}$ and $\mathbf{L^2}$ show good activity against both parasite strains, with the IC_{50}-values for $\mathbf{L^1}$ (against D10) being just above those for chloroquine. Ligand $\mathbf{L^4}$ exhibited medium activity against both strains (resistance index, RI = 1.0, cf. Table 2), while $\mathbf{L^3}$ was active against the chloroquine sensitive (CQS) strain, but inactive against the chloroquine resistant (CQR) strain. Complexes **1** and **2** showed medium activity against D10 (CQS) and 3–4 times lower activity against Dd2 (CQR, relative to D10), while complex **3** is very active against the CQS strain, though less active against the CQR strain. The complexes and ligands were screened for cytotoxicity against a mammalian cell line, Chinese Hamster Ovarian (CHO), with emetine as reference drug. Ligands $\mathbf{L^1}$ and $\mathbf{L^2}$ showed low cytotoxicity (IC_{50} = 144 μM and IC_{50} = 240 μM, Table 2), while $\mathbf{L^3}$ and $\mathbf{L^4}$ showed no measurable cytotoxicity at the highest tested concentration. Correspondingly, complexes **1** and **2** also showed no cytotoxicity at the highest tested concentration. Complex **3** showed higher cytotoxicity than the other two complexes (IC_{50} = 89 μM). In summary, all tested samples exhibited low or no cytotoxicity.

Ligands $\mathbf{L^1}$ [54] and $\mathbf{L^2}$ both show promising antimalarial activity, even though they are less active than chloroquine against the CQR strain. Ligand $\mathbf{L^2}$ is previously unreported and exhibits very low toxicity against mammalian cells (Selectivity index = 1263, cf. Table 2). Compared to the corresponding ligands, the complexes [RuCl(*p*-cymene)(L)]Cl (L = $\mathbf{L^1}$ (**1**); $\mathbf{L^2}$ (**2**)) had significantly lower antimalarial activity. This is not surprising, since by blocking two of the nitrogens of the ligand, the ruthenium fragment in **1** and **2** might impede the ability of the complexes to accumulate in the food vacuole, resulting in low activity. However, for complex [RuCl(*p*-cymene)($\mathbf{L^3}$)] (**3**) the relationship is reversed; the activity of the complex is notably higher than that of the ligand. The resistance index for **3** is high (RI = 18), but this is most likely a consequence of the lack of activity against the CQR strain for $\mathbf{L^3}$. The activity of **3** is considerably higher than that of **1** and **2** (particularly against the CQS strain). Conductivity data (*vide supra*) suggest that the behaviour of **3** in aqueous solution differs slightly from that of **1** and **2**, which might be related to activity.

Even though firm conclusions cannot be drawn based on results from two parasite strains, a few points are worth noticing regarding the cross-resistance with chloroquine of the reported

complexes and ligands.[55] Ligand **L^1** is fully cross-resistant with chloroquine, but exchange of the terminal pyridine group for a methylimidazole as in **L^2** results in a compound that is not cross-resistant. Most notable is the very high resistance of the Dd2 strain to **L^3**, which could suggest that **L^3** is transported out of the food vacuole of the parasite to a higher extent than the other ligands. The level of resistance to **L^3** is only partly decreased by metal complexation. These results suggest that coordination to a metal atom may limit cross-resistance with chloroquine, but does not necessarily eliminate it. More importantly, the antimalarial activity data of **L^3** and **3** indicates that attachment of the bulky metal group to **L^3** does not prevent interaction with the chloroquine resistance transporter, PfCRT. The limited number of ligands and corresponding ruthenium arene complexes prevents a clear correlation between structure and cross-resistance.

Heme aggregation inhibition activity (HAIA) and water-octanol distribution coefficients

As mentioned in the introduction, the design of new antiplasmodial agents aimed at overcoming chloroquine resistance must take into consideration the heme aggregation inhibition activity (HAIA), as well as relevant physicochemical factors, such as lipophilicity. The antimalarial potential of the Ru-chloroquine complexes depicted in Fig. 1 against resistant strains of the *Plasmodium falciparum* parasite has been demonstrated.[41,56] The incorporation of a metal centre induced important structural modifications together with an increase in the lipophilicity of the drug and an enhancement of the $HAIR_{50}$ values (drug to hemin ratio required to inhibit 50% of heme aggregation). This combination of features were claimed to be responsible for the high activity observed against resistant parasites. However, complexation of the metal to chloroquine (CQ) in those cases took place through the quinoline nitrogen, which resulted in an undesirable decreased basicity of the new drugs, a crucial property for pH trapping in the acidic vacuole. In the new series of complexes reported herein, Ru(II) is coordinated to the chloroquine analogues in a way that does not block the basic quinoline nitrogen, while the enhancement of the lipophilicity compared to the free ligand is still possible, and they were thus expected to display interesting biological properties. It was therefore important to gather experimental data on the above-mentioned physicochemical features of the new compounds.

The results of water-octanol distribution coefficients (D) as a measure of lipophilicity, and $HAIR_{50}$ measurements are shown in Table 3 for the ligands and metal complexes, in comparison with chloroquine. Most of the ligands and their Ru complexes display an increased lipophilicity at the acidic conditions of the digestive vacuole (pH 4.9) with respect to chloroquine, which might be a good indicator of activity against resistant parasites. On the other hand, **L^1** shows similar lipophilicity to chloroquine, whereas **2** is clearly more hydrophilic. Moreover, with the only exception of **L^3**, all the ligands and the corresponding metal complexes are more than twice as potent as chloroquine in their HAIA ability at an aqueous acetate/n-octanol interface,[41] as seen by the values of $HAIR_{50}$. Interestingly, the HAIA ability is also enhanced with reference to the Ru-chloroquine complexes previously described by us (Fig. 1),[41,56] again with the sole exception of **L^3**.

Due to the high number of variables introduced in the design of the new drug candidates tested (presence or absence of metal moiety, charge and/or substantially different structural features) an internal correlation among the new family of chloroquine analogues and/or their metal complexes regarding the HAIA ability and lipophilicity is not obvious. However, it may be noted that complexation to the metal did not induce a significant modification of the HAIA or an increase in lipophilicity at pH 4.9 of the ligands in the pairs **L^1-1**, **L^2-2**, contrary to what was previously observed for other Ru-CQ drug candidates,[41,56] and contrary to the results obtained for **L^3-3**.Furthermore, no clear correlations were found between $HAIR_{50}$ or lipophilicity with the antiplasmodial activity against CQS or CQR *Plasmodium falciparum* parasites. Again, this is most likely a consequence of the complexity of the systems, i.e. the

fact that the final antimalarial activity is the result of a multifaceted balance of heme aggregation inhibition activity, lipophilicity, structural features, solubility and general pharmacokinetic behaviour when the drug candidates are within biological systems. However, it is again worth noting the case of $\mathbf{L^3}$ and **3**. The complexation of an *inactive* ligand, which results in a notable increase of the HAIA ability at the interface and a slight increase of lipophilicity at the acidic vacuole conditions, gives a metal compound with a significantly enhanced antimalarial activity. This indicates that, for the series of compounds reported herein, only when the incorporation of a metal moiety induces important changes in the lipophilicity and/or the HAIA ability of an *inactive* ligand, there is a good correlation with the differences observed in the final overall antiplasmodial activity of the complex.

Another feature which might contribute to the increased activity of **3** relative to $\mathbf{L^3}$ is aqueous solubility at physiological pH. Coordination to an arene metal unit as a means to increasing aqueous solubility and bioavailability of ligands with known biological activity has been documented in the literature.[42,57] Even though lipophilicity at vacuolar pH increases upon coordination of $\mathbf{L^3}$ to the metal fragment, lipophilicity at pH 6.6 decreases. As $\mathbf{L^3}$ is virtually insoluble in water at neutral pH, the increased aqueous solubility of **3** could be one of the factors involved in the higher antimalarial activity.

Conclusion

A small family of ruthenium arene half sandwich complexes with chloroquine analogue ligands was synthesized and characterized by NMR spectroscopy, mass spectrometry and, in one case, X-ray crystallography. These complexes differ from previously reported ruthenium complexes with antimalarial activity, as the quinoline group is pendant, leaving the quinoline nitrogen uncoordinated. In the case of the ligands $\mathbf{L^1}$ and $\mathbf{L^2}$, coordination to the metal fragment did not result in increased antimalarial activity, but these ligands themselves displayed significant activity. However, complex **3** was considerably more active than $\mathbf{L^3}$ and showed good activity, particularly against the chloroquine sensitive strain of *P. falciparum*. The lipophilicity and heme aggregation inhibition activity at an aqueous buffer/n-octanol interface ($HAIR_{50}$) were measured for all ligands and complexes but a general correlation with the *in vitro* antimalarial activity could not be established. In the case of the $\mathbf{L^3}$**-3** couple, the enhancement of the antiplasmodial activity upon coordination to a metal centre was related to an increase in lipophilicity and the HAIA ability at the buffer/n-octanol interface. The high antimalarial activity of **3** is a promising result that warrants more research, including further study of the structure activity relationships of (η^6-arene)Ru complexes with bidentate chloroquine analogue ligands. It is conceivable that structural optimization of $\mathbf{L^3}$ could give a complex with high activity also against chloroquine resistant strains.

Experimental

General

All synthetic procedures were performed under dry nitrogen using standard Schlenk and vacuum-line techniques. Solvents used were dried by distillation over appropriate drying reagents and stored over molecular sieves under nitrogen. All chemicals were purchased from Sigma Aldrich and used as received. $[(p\text{-cymene})RuCl_2]_2$[58] and N^1-(7-chloroquinolin-4-yl)ethane-1,2-diamine[59] were prepared according to literature methods. NMR spectra were recorded on a Varian Inova 500 MHz spectrometer using the solvent resonance as internal standard for ^1H NMR and ^{13}C NMR shifts. Infrared spectra were recorded on a Nicolet Avatar 360 FT-IR spectrometer. Electrospray ionization (ESI) and high resolution mass spectra were recorded using a Waters Micromass Q-Tof micro mass spectrometer or an LC-MS Agilent 6220-TOF coupled with 1200 series HPLC.

Conductivity values were obtained using 1 mM solutions of the complexes in water or DMSO at various time intervals using an Oaklon pH/Conductivity meter. Elemental analysis was performed by Mikroanalytische Laboratorium Kolbe, Mülheim an der Ruhr.

X-ray Structure Determinations

The crystal was immersed in cryo-oil, mounted in a Nylon loop, and measured at a temperature of 100 K. The X-ray diffraction data were collected on a Bruker AXS Kappa ApexII Duo diffractometer using Mo Kα radiation (λ= 0.71073 Å). The *APEX2*[60] program package was used for cell refinements and data reductions. The structures were solved by direct methods using *SHELXS-97*.[61] A semi-empirical absorption correction based on equivalent reflections (*SADABS*)[62] was applied to the data. Structural refinements were carried out using *SHELXL-97*.[61] The NH hydrogen atoms were located from the difference Fourier map but constrained to ride on their parent atom, with $U_{iso} = 1.5 \cdot U_{eq}$(parent atom). Other hydrogen atoms were positioned geometrically and were also constrained to ride on their parent atoms, with C–H = 0.95–1.00 Å, and $U_{iso} = 1.2–1.5 \cdot U_{eq}$(parent atom). The crystallographic details are summarized in Table 1.

Syntheses

***N*-(2-((pyridin-2-yl)methylamino)ethyl)-7-chloroquinolin-4-amine (L^1)—**N^1-(7-chloroquinolin-4-yl)ethane-1,2-diamine (0.800 g, 3.6 mmol) was dissolved in methanol (30 mL). 2-pyridinecarboxaldehyde (0.34 mL, 3.6 mmol) was added dropwise and the solution was stirred for 16 h at room temperature. Sodium borohydride (0.272 g, 7.2 mmol) was added and the reaction mixture was stirred for an additional hour. The solvent was removed *in vacuo* and the residue was dissolved in EtOAc (150 mL). The organic phase was washed with brine (3×50 mL), dried over Na_2SO_4 and evaporated. The product was purified by silica gel flash chromatography eluting with ethyl acetate-methanol-triethylamine 8:1:1 (v/v). Product was obtained as a beige solid (0.876g, 81%). ^{1}H NMR (500 MHz, $CDCl_3$) δ 8.58 (d, 1H, J=4.4Hz), 8.52 (d, 1H, J=5.3Hz), 7.95 (d, 1H, J=2.1Hz), 7.81 (d, 1H, J=8.9Hz), 7.65 (dt, 1H, J=1.7Hz, J=7.7Hz), 7.36 (dd, 1H, J=2.1Hz, J=8.9Hz), 7.27 (d, 1H, J=8.0Hz), 7.19 (dd, 1H, J=5.1Hz, J=6.7Hz), 6.38 (d, 1H, J=5.4Hz), 6.09 (br s, 1H), 3.99 (s, 2H), 3.37 (m, 2H), 3.08 (m, 2H), 2.05 (br s, 1H); ^{13}C NMR (125 MHz, $CDCl_3$) δ 159.2, 151.9, 150.0, 149.3, 149.0, 136.6, 134.8, 128.5, 125.1, 122.4, 122.2, 121.5, 117.4, 99.1, 54.2, 47.0, 42.3; IR (KBr) ν_{max}/cm^{-1} 3221m (br), 3067w, 2962w, 2839w, 1613m (7-chloroquinoline), 1582s (7-chloroquinoline), 1452m, 1431m, 1380m, 1333w, 1282w, 1249w, 1204w, 1140w, 1112w, 1082w, 849w, 807w, 763m; HRMS (ES+) *m/z* calcd. for $C_{17}H_{18}N_4Cl$ 313.12145, found 313.12215.

***N*-(2-((1-methyl-1H-imidazol-2-yl)methylamino)ethyl)-7-chloroquinolin-4-amine (L^2)—**N^1-(7-chloroquinolin-4-yl)ethane-1,2-diamine (0.300 g, 1.35 mmol) and 1-methyl-2-imidazole carboxaldehyde (0.150 g, 1.35 mmol) were dissolved in methanol (30 mL) and a few molecular sieves (3Å) were added. The solution was stirred for 18 h at room temperature. Sodium borohydride (0.102 g, 2.7 mmol) was added and the reaction mixture was stirred for an additional hour. Molecular sieves were filtered off and the solvent was removed *in vacuo*. The residue was dissolved in EtOAc (50 mL). The organic phase was washed with brine (3×25 mL), dried over Na_2SO_4 and evaporated. Product was obtained as a white/yellow solid (0.396g, 92%). ^{1}H NMR (500 MHz, CD_3OD) δ 8.34 (d, 1H, J=5.6Hz), 8.09 (d, 1H, J=9.0Hz), 7.77 (d, 1H, J=2.1Hz), 7.39 (dd, 1H, J=2.2Hz, J=9.0Hz), 6.98 (d, 1H, J=1.3Hz), 6.86 (d, 1H, J=1.3Hz), 6.52 (d, 1H, J=5.7Hz), 3.90 (s, 2H), 3.68 (s, 3H), 3.46 (t, 2H, J=6.3Hz), 2.96 (t, 2H, J=6.3Hz); ^{13}C NMR (125 MHz, CD_3OD) δ 152.8, 152.5, 149.7, 147.6, 136.4, 127.6, 127.1, 126.1, 124.4, 123.0, 118.8, 99.8, 47.9, 45.2, 43.5, 33.1; IR (KBr) ν_{max}/cm^{-1} 3260m (br), 3255m, 3063w, 2961w, 2832w, 1613m (7-chloroquinoline), 1581s (7-chloroquinoline), 1549m (7-chloroquinoline), 1452m, 1429m, 1376m, 1289m, 1250w,

1216w, 1138m, 1106m, 1082w, 960w, 852m, 812w, 729m; HRMS (ES+) *m/z* calcd. for $C_{16}H_{19}N_5Cl$ 316.1329, found 316.1340.

***N*-(2-((2-hydroxyphenyl)methylimino)ethyl)-7-chloroquinolin-4-amine (L^3)—**N^1-(7-chloroquinolin-4-yl)ethane-1,2-diamine (2.026 g, 9.14 mmol) was dissolved in ethanol (90 mL). Salicylaldehyde (0.95 mL, 8.96 mmol) was added dropwise and the solution was stirred at room temperature for 45 min. The solvent was evaporated and the residue was washed with cold ethanol and petroleum ether. The product was obtained as a yellow solid (2.24 g, 77%). ^{1}H NMR (500 MHz, $CDCl_3$) δ 12.99 (br s, 1H), 8.58 (d, 1H, J=5.3Hz), 8.37 (s, 1H), 7.97 (d, 1H, J=0.9Hz), 7.60 (d, 1H, J=8.9Hz), 7.36 (m, 2H), 7.22 (d, 1H, J=7.5Hz), 6.98 (d, 1H, J=8.3Hz), 6.89 (t, 1H, J=7.5Hz), 6.51 (d, 1H, J=5.3Hz), 5.20 (br s, 1H), 3.95 (m, 2H), 3.74 (m, 2H); ^{13}C NMR (125 MHz, $CDCl_3$) δ 167.2, 160.9, 152.0, 149.2, 149.1, 135.1, 132.8, 131.6, 129.0, 125.7, 120.7, 119.0, 118.5, 117.2, 117.1, 99.3, 57.7, 43.5; IR (KBr) ν_{max}/cm^{-1} 3405s (O–H), 2940w, 2855w, 1630m (N=C), 1613m (7-chloroquinoline), 1578s (7-chloroquinoline), 1541w (7-chloroquinoline), 1508w, 1449w, 1425w, 1379w, 1278m, 1210w, 1143w, 895w, 761m; HRMS (ES+) *m/z* calcd. for $C_{18}H_{17}N_3OCl$ 326.1060, found 326.1059.

***N*-(2-(bis((pyridin-2-yl)methyl)amino)ethyl)-7-chloroquinolin-4-amine (L^4)—**N^1-(7-chloroquinolin-4-yl)ethane-1,2-diamine (0.200g, 0.9 mmol) was dissolved in dichloromethane (12 mL). 2-pyridinecarboxaldehyde (0.17 mL, 1.8 mmol) was added dropwise and the solution was stirred at room temperature for 30 min. Sodium tris(acetoxy)borohydride (0.900g, 4.1 mmol) was added and the reaction mixture was stirred for 17 h. A second portion of sodium triacetoxyborohydride (0.290 g, 1.3 mmol) was added and the stirring was continued for 3 h. Saturated aqueous Na_2CO_3 (7 mL) was added and when gas evolution subsided, the organic phase was washed with additional aqueous Na_2CO_3 (2×10 mL). The organic phase was dried over Na_2SO_4 and evaporated. The crude product was purified by silica gel flash chromatography eluting with ethyl acetate-methanol-triethylamine 83:07:10 (v/v). The pure product was obtained as a brown oil (0.221 g, 61%). ^{1}H NMR (500 MHz, $CDCl_3$) δ 8.57 (ddd, 2H, J=0.8Hz, J=1.6Hz, J=4.9Hz), 8.46 (d, 1H, J=5.4Hz), 8.32 (d, 1H, J=9.0Hz), 7.97 (d, 1H, J=2.1Hz), 7.56 (dt, 2H, J=1.8Hz, J=7.7Hz), 7.48 (br s, 1H), 7.45 (dd, 1H, J=2.2Hz, J=8.9Hz), 7.36 (d, 2H, J=7.8Hz), 7.15 (ddd, 2H, J=1.0Hz, J=4.9Hz, J=7.4Hz), 6.25 (d, 1H, J=5.5Hz), 3.97 (s, 4H), 3.30 (m, 2H), 3.00 (m, 2H); ^{13}C NMR (125 MHz, $CDCl_3$) δ 158.9, 151.9, 149.8, 149.2, 149.0, 136.6, 134.3, 128.3, 124.9, 123.2, 122.5, 122.3, 117.7, 98.7, 59.8, 51.1, 40.5; IR (KBr) ν_{max}/cm^{-1} 3199m (br), 3058m, 3006m, 2942w, 1611m (7-chloroquinoline), 1581s (7-chloroquinoline), 1546m (7-chloroquinoline), 1449w, 1433m, 1367w, 1283w, 1226m, 1150m, 1076w, 850w, 759m; HRMS (ES+) *m/z* calcd. for $C_{23}H_{23}N_5Cl$ 404.16365, found 404.16356.

(η^6-*p*-cymene)(*N*-(2-((pyridin-2-yl)methylamino)ethyl)-7-chloroquinolin-4-amine)chlororuthenium(II) chloride, [RuCl(cymene)(L^1)]Cl (1)—[(*p*-cymene)$RuCl_2]_2$ (0.200 g, 0.32 mmol) and $\mathbf{L^1}$ (0.204 g, 0.64 mmol) were dissolved in dichloromethane (20 mL) and stirred at room temperature overnight. The solvent volume was reduced to approx. 3 mL and the product was precipitated with diethyl ether. The product was isolated via filtration and washed with diethyl ether and petroleum ether. The product was obtained as a fine, yellow solid (0.357g, 91%). ^{1}H NMR (500 MHz, $CDCl_3$) δ 9.56 (br s, 1H), 8.98 (d, 1H, J=9.1Hz), 8.89 (d, 1H, J=5.2Hz), 8.52 (d, 1H, J=5.4Hz), 8.10 (br s, 1H), 7.95 (d, 1H, J=0.8Hz), 7.83 (dt, 1H, J=1.4Hz, J=7.8Hz), 7.52 (dd, 1H, J=2.1Hz, J=9.0Hz), 7.40 (t, 1H, J=6.9Hz), 7.30 (d, 1H, J=7.7Hz), 6.33 (d, 1H, J=5.4Hz), 5.98 (d, 1H, J=5.9Hz), 5.91 (d, 1H, J=6.1Hz), 5.55 (d, 1H, J=6.0Hz), 5.39 (d, 1H, J=6.1Hz), 4.62 (dd, 1H, J=6.1Hz, J=16.1Hz), 3.93 (dd, 1H, J=5.4Hz, J=16.2Hz), 3.62 (m, 2H), 3.56 (m, 1H), 3.13 (m, 1H), 2.78 (hept, 1H, J=6.9Hz), 2.04 (s, 3H), 1.08 (d, 3H, J=7.0Hz), 1.02 (d, 3H,

J=6.9Hz); ^{13}C NMR (125 MHz, $CDCl_3$) δ 161.2, 153.6, 151.4, 150.3, 149.0, 139.2, 135.3, 127.6, 125.7, 125.1, 124.9, 121.8, 117.9, 105.7, 98.3, 97.1, 84.7, 84.3, 83.9, 82.8, 58.7, 53.7, 41.1, 30.8, 22.6, 21.4, 18.0; IR (KBr) ν_{max}/cm^{-1} 3410m (br), 3060w, 2964w, 1610m (7-chloroquinoline), 1580s (7-chloroquinoline), 1535w (7-chloroquinoline), 1451m, 1372w, 1330w, 1141w, 1088w, 765w; MS (ES+) *m/z* 583 (M^+, 100%), 548 (30, MH - Cl); HRMS (ES+) *m/z* calcd. for $C_{27}H_{31}N_4Cl_2Ru$ 583.0969, found 583.0985; Elemental analysis (%) calcd. for $C_{27}H_{31}N_4Cl_3Ru{\cdot}0.8CH_2Cl_2$: C 48.61, H 4.78, N 8.16, found: C 48.65, H 4.83, N 8.29.

(η^6-*p*-cymene)(*N*-(2-((1-methyl-1H-imidazol-2-yl)methylamino)ethyl)-7-chloroquinolin-4-amine)chlororuthenium(II) chloride, [RuCl(cymene)(L^2)]Cl (2)—This compound was synthesized from [(*p*-cymene)$RuCl_2]_2$ (0.100 g, 0.16 mmol) and **L^2** (0.103 g, 0.32 mmol) using the same procedure employed for synthesis of **1** (*vide supra*). The product was obtained as a fine, yellow solid (0.192 g, 95%). ^{1}H NMR (500 MHz, $CDCl_3$) δ 9.09 (br s, 1H), 8.99 (d, 1H, J=9.0Hz), 8.54 (d, 1H, J=5.4Hz), 8.34 (br s, 1H), 7.96 (d, 1H, J=2.1Hz), 7.50 (dd, 1H, J=2.2Hz, J=9.0Hz), 7.20 (d, 1H, J=1.6Hz), 6.91 (d, 1H, J=1.5Hz), 6.36 (d, 1H, J=5.5Hz), 5.87 (d, 1H, J=5.6Hz), 5.55 (d, 1H, J=6.0Hz), 5.36 (d, 1H, J=6.1Hz), 5.28 (d, 1H, J=5.7Hz), 4.27 (m, 1H), 3.91 (m, 1H), 3.65 (m, 3H), 3.57 (s, 3H), 3.45 (m, 1H), 2.89 (hept, 1H, J=6.9Hz), 2.14 (s, 3H), 1.19 (d, 3H, J=6.9Hz), 1.16 (d, 3H, J=7.0Hz); ^{13}C NMR (125 MHz, $CDCl_3$) δ 151.2, 150.3, 149.6, 148.9, 135.5, 128.1, 127.6, 125.8, 125.1, 123.0, 117.9, 106.0, 98.1, 96.1, 83.2, 82.6, 81.0, 55.4, 46.2, 41.0, 34.8, 30.9, 22.9, 21.3, 18.1; IR (KBr) ν_{max}/cm^{-1} 3411m, 3258m, 3092w, 2964w, 2867w, 1612w (7-chloroquinoline), 1579s (7-chloroquinoline), 1538w (7-chloroquinoline), 1513w, 1451m, 1421, 1363, 1327, 1138w, 1088w, 869w; HRMS (ES+) *m/z* calcd. for $C_{26}H_{32}N_5Cl_2Ru$ 586.1078, found 586.1077; Elemental analysis (%) calcd. for $C_{26}H_{32}N_5Cl_3Ru{\cdot}0.6CH_2Cl_2$: C 47.47, H 4.97, N 10.41, found: C 47.47, H 5.02, N 10.14.

(η^6-*p*-cymene)(*N*-(2-((2-hydroxyphenyl)methylimino)ethyl)-7-chloroquinolin-4-amine)chlororuthenium(II), [RuCl(cymene)(L^3)] (3)—L^3 (0.053 g, 0.16 mmol) was dissolved in dichloromethane (10 mL) and triethylamine (0.023 mL, 0.16 mmol) was added. The solution was stirred at room temperature for 30 min and [(*p*-cymene)$RuCl_2]_2$ (0.050 g, 0.08 mmol) was added. Stirring at ambient temperature continued overnight. The solvent volume was reduced to approx. 2 mL and the product was precipitated with diethyl ether. The precipitate was isolated via filtration and washed with water (2–3 mL), diethyl ether and petroleum ether. The product was dried under vacuum and obtained as an orange solid (0.065 g, 67%). ^{1}H NMR (500 MHz, $CDCl_3$) δ 8.37 (d, 1H, J=4.3Hz), 8.02 (d, 1H, J=1.5Hz), 7.85 (d, 1H, J=9.0Hz), 7.51 (br s, 1H), 7.39 (s, 1H), 7.22 (dd, 1H, J=1.5Hz, J=9.1Hz), 7.15 (m, 1H), 6.91 (d, 1H, J=8.5Hz), 6.55 (d, 1H, J=3.9Hz), 6.48 (d, 1H, J=7.7Hz), 6.27 (t, 1H, J=7.3Hz), 5.57 (d, 1H, J=6.2Hz), 5.52 (d, 1H, J=6.2Hz), 5.46 (d, 1H, J=5.4Hz), 5.09 (d, 1H, J=5.4Hz), 4.57 (m, 1H), 4.27 (m, 2H), 3.97 (m, 1H), 2.75 (hept, 1H, J=6.9Hz), 2.29 (s, 3H), 1.24 (d, 3H, J=6.9Hz), 1.14 (d, 3H, J=6.9Hz); ^{13}C NMR (125 MHz, $CDCl_3$) δ 166.0, 165.0, 154.8, 143.1, 139.5, 139.2, 135.6, 134.9, 127.8, 124.7, 122.1, 120.3, 118.6, 115.4, 114.7, 100.9, 98.8, 98.5, 87.7, 83.1, 81.2, 80.6, 44.8, 43.8, 30.6, 22.9, 21.6, 18.9; IR (KBr) ν_{max}/cm^{-1} 3422m (br), 3236m, 3056w, 2961w, 1615s (7-chloroquinoline), 1587m (7-chloroquinoline), 1536w (7-chloroquinoline), 1467m, 1449m, 1318w, 1213w, 1146w, 1091w, 1018w, 877w, 758w; MS (ES+) *m/z* 596 (M+H, 100%), 560 (25, M-HCl); HRMS (ES+) *m/z* calcd. for $C_{28}H_{30}N_3Cl_2ORu$ 596.0809, found 596.0822.

Heme Aggregation Inhibition Activity (HAIA) at a water/n-octanol interface

Inhibition of the heme aggregation near the interface of aqueous buffer/ n-octanol mixtures was studied following a previously published method.[41] To establish a base line for the aggregation process, hemin was dissolved in 0.1 M NaOH solution to generate hematin and

acetone was added until the acetone:water ratio was 4:6; the final solution contained 15 mg hematin/ml. A sample of this solution (200 μl) was carefully introduced close to the interface between n-octanol (2 ml) and aqueous acetate buffer (5 ml; pH 4.9) in a cylindrical vial with an internal diameter of 2.5 cm. The mixture was incubated at 37 °C for 60 min and at the end of the incubation period it was stirred to ensure the transfer of all solid particles to the aqueous layer. The product (β-hematin) was isolated by centrifugation. The pellet was collected and washed with DMSO (4 ml), centrifuged again for 20 min, washed with 2 ml of ethanol and finally dissolved in 25 ml of 0.1 M NaOH for spectrophotometric quantification. For the aggregation inhibition activity measurements the appropriate amount of each drug (23 mM in n-octanol) to yield [drug]:[hemin] ratios in the range 1–6 was added to the acetate buffer/n-octanol mixture; after stirring for 30 min to equilibrate the drug between the two phases, the hematin solution was added close to the interface and the procedure was followed as described above. All experiments were performed in quadruplicate.

Determination of Partition Coefficients

The distribution of all complexes between n-octanol and water was studied by use of the stir-flask method.[63–65] A mixture of 10 ml n-octanol and 10 ml of water (each saturated in the other) was stirred for 30 min at the desired temperature after adding the right amount of the sample to be analyzed (~ 0.7 mmol). The pH was adjusted to the desired value by addition of either a 0.1 M solution of H_3PO_4 or NaOH (10–20 μl). Once the equilibrium was reached, the organic and aqueous phases were separated and centrifuged. Finally, the concentration of drug in each phase was measured spectrophotometrically in order to determine values of D = [drug](in n-octanol)/[drug](in water). Experiments were carried out in quadruplicate.

Determination of *in vitro* antiplasmodial activity

Two strains of *Plasmodium falciparum* were used in this study - the chloroquine sensitive strain D10 and the chloroquine resistant strain Dd2. Continuous *in vitro* cultures of asexual erythrocyte stages of *P. falciparum* were maintained using a modified method of Trager and Jensen.[66] Quantitative assessment of antiplasmodial activity *in vitro* was determined via the parasite lactate dehydrogenase assay using a modified method described by Makler.[67] The test samples were tested in triplicate on one occasion. The test samples were prepared as a 20 mg/ml stock solution in 100% DMSO. Samples were tested as a suspension if not completely dissolved. Stock solutions were stored at −20°C. Further dilutions were prepared on the day of the experiment. Chloroquine (CQ) was used as the reference drug in all experiments. A full dose-response was performed for all compounds to determine the concentration inhibiting 50% of parasite growth (IC_{50}–value). Test samples **1** and **2** were tested at a starting concentration of 100 μg/ml, which was then serially diluted 2-fold in complete medium to give 10 concentrations; with the lowest concentration being 0.2 μg/ml. The same dilution technique was used for all samples. Test samples $\mathbf{L^3}$ and $\mathbf{L^4}$ were tested at a starting concentration of 10 μg/ml. Test samples $\mathbf{L^1}$ and **3** were tested at a starting concentration of 1000 ng/ml. Test sample $\mathbf{L^2}$ was tested at a starting concentration of 100 ng/ml against the CQS strain and 1000 ng/ml against the CQR strain. CQ was tested at a starting concentration of 100 ng/ml against the CQS strain and 1000 ng/ml against the CQR strain. The highest concentration of solvent to which the parasites were exposed to had no measurable effect on the parasite viability (data not shown).

Cytotoxicity assay

Cytotoxicity was assessed against a Chinese Hamster Ovarian (CHO) cell line using the 3-(4,5-dimethylthiazol-2yl)-2,5-diphenyltetrazoliumbromide (MTT) assay.[68] The test samples were tested in triplicate on one occasion. The test samples were prepared as a 20 mg/ml stock solution in 100% DMSO. Dilutions were prepared on the day of the experiment.

Emetine was used as the reference drug in all experiments. The initial concentration of emetine was 100 μg/mL, which was serially diluted in complete medium with 10-fold dilutions to give six concentrations, the lowest being 0.001 μg/mL. The same dilution technique was applied to all the test samples. The highest concentration of solvent to which the cells were exposed had no measurable effect on the cell viability (data not shown). The 50% inhibitory concentration (IC50) values were obtained from full dose-response curves, using a nonlinear dose-response curve fitting analysis via Graph Pad Prism v.4.0 software.

Acknowledgments

This research has been funded by the Swedish International Development Cooperation Agency (SIDA) and the Swedish Research Council (VR). Financial support from the NIH through Grant # 5SC1GM89558-2 to R.A. S.-D. is gratefully acknowledged.

References

1. Carter R, Mendis KN. Clin. Microbiol. Rev. 2002; 15:564–594. [PubMed: 12364370]
2. WHO Malaria Report 2009. http://www.who.int/malaria/world_malaria_report_2009.
3. Dondorp AM, Yeung S, White L, Nguon C, Day NPJ, Socheat D, von Seidlein L. Nat. Rev. Microbiol. 2010; 8:272–280. [PubMed: 20208550]
4. Dondorp AM, Nosten F, Yi P, Das D, Phyo AP, Tarning J, Lwin KM, Ariey F, Hanpithakpong W, Lee SJ, Ringwald P, Silamut K, Imwong M, Chotivanich K, Lim P, Herdman T, An SS, Yeung S, Singhasivanon P, Day NPJ, Lindegardh N, Socheat D, White NJ. N. Engl. J. Med. 2009; 361:455–467. [PubMed: 19641202]
5. Hastings IM, Bray PG, Ward SA. Science. 2002; 45:2001–2002.
6. Ursos LMB, Roepe PD. Med. Res. Rev. 2002; 22:465–491. [PubMed: 12210555]
7. de Villiers KA, Egan TJ. Molecules. 2009; 14:2868–2887. [PubMed: 19701131]
8. Egan TJ, Marques HM. Coord. Chem. Rev. 1999; 190–192:493–517.
9. Leed A, DuBay K, Ursos LMB, Sears D, De Dios AC, Roepe PD. Biochemistry. 2002; 41:10245–10255. [PubMed: 12162739]
10. Rosenthal, PJ., editor. Antimalarial Chemotherapy: mechanism of action, resistance and new directions in drug discovery. New Jersey: Humana Press; 2001.
11. Chong CR, Sullivan DJ. Biochem. Pharmacol. 2003; 66:2201–2212. [PubMed: 14609745]
12. Egan TJ, Hunter R, Kaschula CH, Marques HM, Misplon A, Walden J. J. Med. Chem. 2000; 43:283–291. [PubMed: 10649984]
13. Cheruku SR, Maiti S, Dorn A, Scorneaux B, Bhattacharjee AK, Ellis WY, Vennerstrom JL. J. Med. Chem. 2003; 46:3166–3169. [PubMed: 12825955]
14. Ridley RG. Nature. 2002; 415:686–693. [PubMed: 11832957]
15. Sanchez CP, McLean JE, Stein W, Lanzer M. Biochemistry. 2004; 43:16365–16373. [PubMed: 15610031]
16. Sanchez CP, McLean JE, Rohrbach P, a Fidock D, Stein WD, Lanzer M. Biochemistry. 2005; 44:9862–9870. [PubMed: 16026158]
17. Roepe PD. Biochemistry. 2011; 50:163–171.
18. van Schalkwyk DA, Egan TJ. Drug Res. Updates. 2006; 9:211–226.
19. Bray PG, Mungthin M, Hastings IM, Biagini GA, Saidu DK, Lakshmanan V, Johnson DJ, Hughes RH, Stocks PA, O'Neill PM, Fidock DA, Warhurst DC, Ward SA. Mol. Microbiol. 2006; 62:238–251. [PubMed: 16956382]
20. Warhurst DC. Malaria J. 2003; 2:31–43.
21. Warhurst D, Craig J, Adagu I, Meyer D, Lee S. Malaria J. 2003; 2:26–30.
22. Egan TJ. J. Inorg. Biochem. 2008; 102:1288–1299. [PubMed: 18226838]
23. Egan TJ. Mol. Biochem. Parasitol. 2008; 157:127–136. [PubMed: 18083247]
24. Hoang AN, Ncokazi KK, a de Villiers K, Wright DW, Egan TJ. Dalton Trans. 2010; 39:1235–1244. [PubMed: 20104349]

25. Biot C, Glorian G, Maciejewski LA, Brocard JS, Domarle O, Blampain G, Millet P, Georges AJ, Lebibi J. J. Med. Chem. 1997; 40:3715–3718. [PubMed: 9371235]
26. http://clinicaltrials.gov/ct2/show/NCT00988507.
27. http://clinicaltrials.gov/ct2/show/NCT00563914.
28. Biot C, Chavain N, Dubar F, Pradines B, Trivelli X, Brocard J, Forfar I, Dive D. J. Organomet. Chem. 2009; 694:845–854.
29. Beagley P, Blackie MAL, Chibale K, Clarkson C, Moss JR, Smith PJ. Dalton Trans. 2002:4426–4433.
30. Beagley P, Blackie MAL, Chibale K, Clarkson C, Meijboom R, Moss JR, Smith PJ, Su H. Dalton Trans. 2003:3046–3051.
31. Sánchez-Delgado RA, Navarro M, Pérez HA, Urbina JA. J. Med. Chem. 1996; 39:1095–1099. [PubMed: 8676344]
32. Navarro M, Pérez HA, Sánchez-Delgado RA. J. Med. Chem. 1997; 40:1937–1939. [PubMed: 9191972]
33. Navarro M, Vásquez F, Sánchez-Delgado RA, Pérez HA, Sinou V, Schrével J. J. Med. Chem. 2004; 47:5204–5209. [PubMed: 15456263]
34. Arancibia R, Dubar F, Pradines B, Forfar I, Dive D, Klahn AH, Biot C. Bioorg. Med. Chem. 2010; 18:8085–8091. [PubMed: 20934349]
35. Glans L, Taylor D, de Kock C, Smith PJ, Haukka M, Moss JR, Nordlander E. J. Inorg. Biochem. 2011; 105:985–990. [PubMed: 21565148]
36. van Rijt SH, Sadler PJ. Drug Discov. Today. 2009; 14:1089–1097. [PubMed: 19782150]
37. Hartinger CG, Dyson PJ. Chem. Soc. Rev. 2009; 38:391–401. [PubMed: 19169456]
38. Süss-Fink G. Dalton Trans. 2010; 39:1673–1688. [PubMed: 20449402]
39. Gasser G, Ott I, Metzler-Nolte N. J. Med. Chem. 2011; 54:3–25. [PubMed: 21077686]
40. Rajapakse CSK, Martínez A, Naoulou B, Jarzecki AA, Suárez L, Deregnaucourt C, Sinou V, Schrével J, Musi E, Ambrosini G, Schwartz GK, Sánchez-Delgado RA. Inorg. Chem. 2009; 48:1122–1131. [PubMed: 19119867]
41. Martínez A, Rajapakse CSK, Jalloh D, Dautriche C, Sánchez-Delgado RA. J. Biol. Inorg. Chem. 2009; 14:863–871. [PubMed: 19343380]
42. Schmid WF, John RO, Mühlgassner G, Heffeter P, Jakupec MA, Galanski M, Berger W, Arion VB, Keppler BK. J. Med. Chem. 2007; 50:6343–6355. [PubMed: 17997519]
43. Carmona D, Lamata MP, Viguri F, Rodríguez R, Lahoz FJ, Dobrinovitch IT, Oro LA. Dalton Trans. 2008:3328–3338. [PubMed: 18560665]
44. Dickson SJ, Paterson MJ, Willans CE, Anderson KM, Steed JW. Chem. Eur. J. 2008; 14:7296–7305. [PubMed: 18613165]
45. Govender P, Renfrew AK, Clavel CM, Dyson PJ, Therrien B, Smith GS. Dalton Trans. 2011; 40:1158–1167. [PubMed: 21165516]
46. Brunner H, Oeschey R, Nuber B. Dalton Trans. 1996:1499–1508.
47. Brunner H, Zwack T, Zabel M, Beck W, Böhm A. Organometallics. 2003; 22:1741–1750.
48. Geary WJ. Coord. Chem. Rev. 1971; 7:81–122.
49. Apelblat A. J. Solution Chem. 2011; 40:1234–1257.
50. Govindaswamy P, Carroll P, Sinha C, Kollipara MR. J. Coord. Chem. 2007; 60:97–107.
51. Mishra H, Mukherjee R. J. Organomet. Chem. 2006; 691:3545–3555.
52. Filak LK, Mühlgassner G, Jakupec MA, Heffeter P, Berger W, Arion VB, Keppler BK. J. Biol. Inorg. Chem. 2010; 15:903–918. [PubMed: 20369265]
53. Grgurić-Sipka S, Ivanović I, Rakić G, Todorović N, Gligorijević N, Radulović S, Arion VB, Keppler BK, Tesić ZL. Eur. J. Med. Chem. 2010; 45:1051–1058. [PubMed: 20053483]
54. Int. Pat. 97/18193. 1997.
55. We thank a reviewer for drawing our attention to these factors relating to the cross-resistance with chloroquine,.
56. Martínez A, Rajapakse CSK, Naoulou B, Kopkalli Y, Davenport L, Sánchez-Delgado RA. J. Biol. Inorg. Chem. 2008; 13:703–712. [PubMed: 18305967]

57. Schmid WF, John RO, Arion VB, Jakupec MA, Keppler BK. Organometallics. 2007; 26:6643–6652.
58. Bennett MA, Smith AK. J. Chem. Soc. Dalton Trans. 1974; 2:233–241.
59. Yearick K, Ekoue-Kovi K, Iwaniuk DP, Natarajan JK, Alumasa J, de Dios AC, Roepe PD, Wolf C. J. Med. Chem. 2008; 51:1995–1998. [PubMed: 18345611]
60. APEX2 - Software Suite for Crystallographic Programs. Madison, Wisconsin, USA: Bruker AXS Inc.; 2009.
61. Sheldrick GM. Acta Crystallogr. Sect. A: Found. Crystallogr. 2008; 64:112–122.
62. Sheldrick, GM. SADABS - Bruker AXS scaling and absorption correction. Madison, Wisconsin, USA: Bruker AXS Inc.; 2008.
63. Danielsson LG, Zhang YH. Trends Anal. Chem. 1996; 15:188–196.
64. Rappel C, Galanski M, Yasemi A, Habala L, Keppler BK. Electrophoresis. 2005; 26:878–884. [PubMed: 15714548]
65. OECD. Guidelines for testing of chemicals. Paris: OECD; 1995.
66. Trager W, Jensen JB. Science. 1976; 193:673–675. [PubMed: 781840]
67. Makler MT, Hinrichs DJ. Am. J. Trop. Med. Hyg. 1993; 48:205–210. [PubMed: 8447524]
68. Mosmann T. J. Immunol. Methods. 1983; 65:55–63. [PubMed: 6606682]

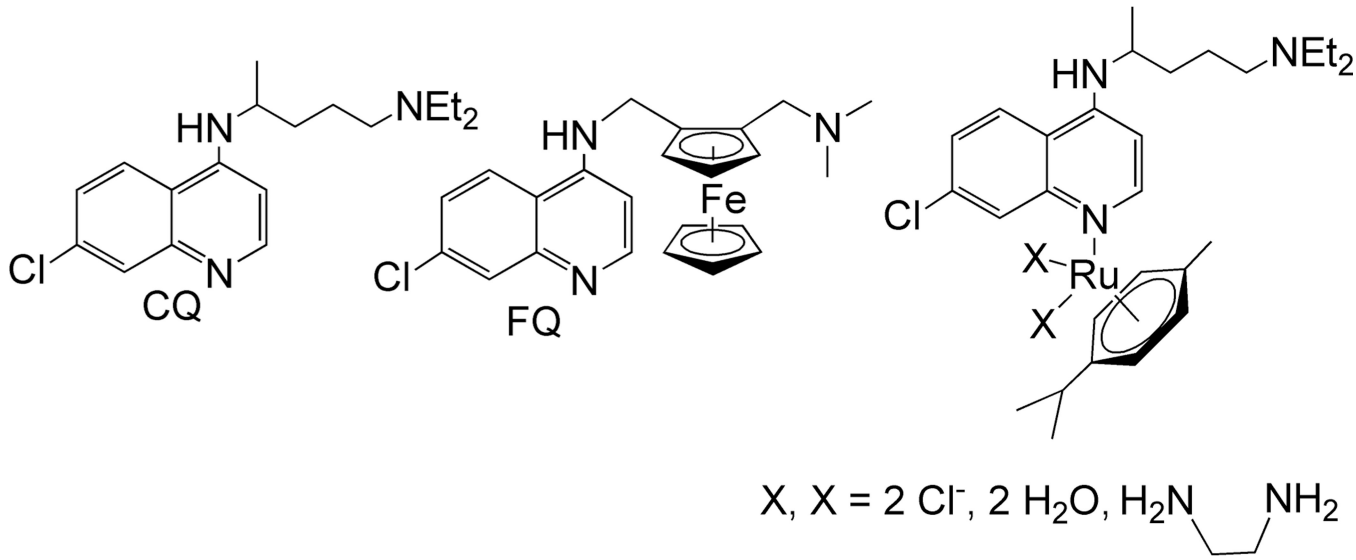

Figure 1.
Structures of chloroquine (CQ), ferroquine (FQ) and reported ruthenium arene complexes with chloroquine as ligand.

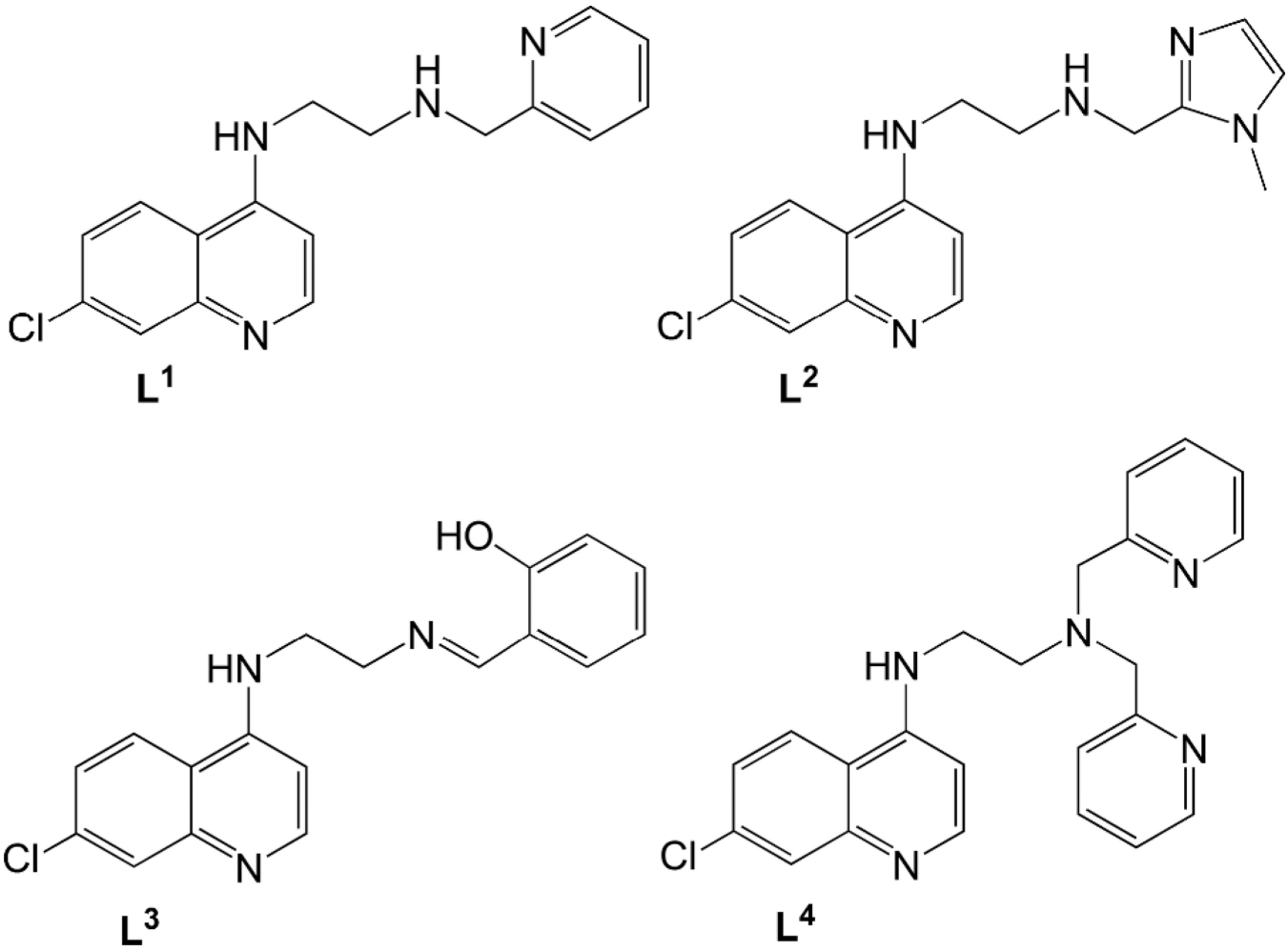

Figure 2.
Structures of ligands **L**[1]–**L**[4].

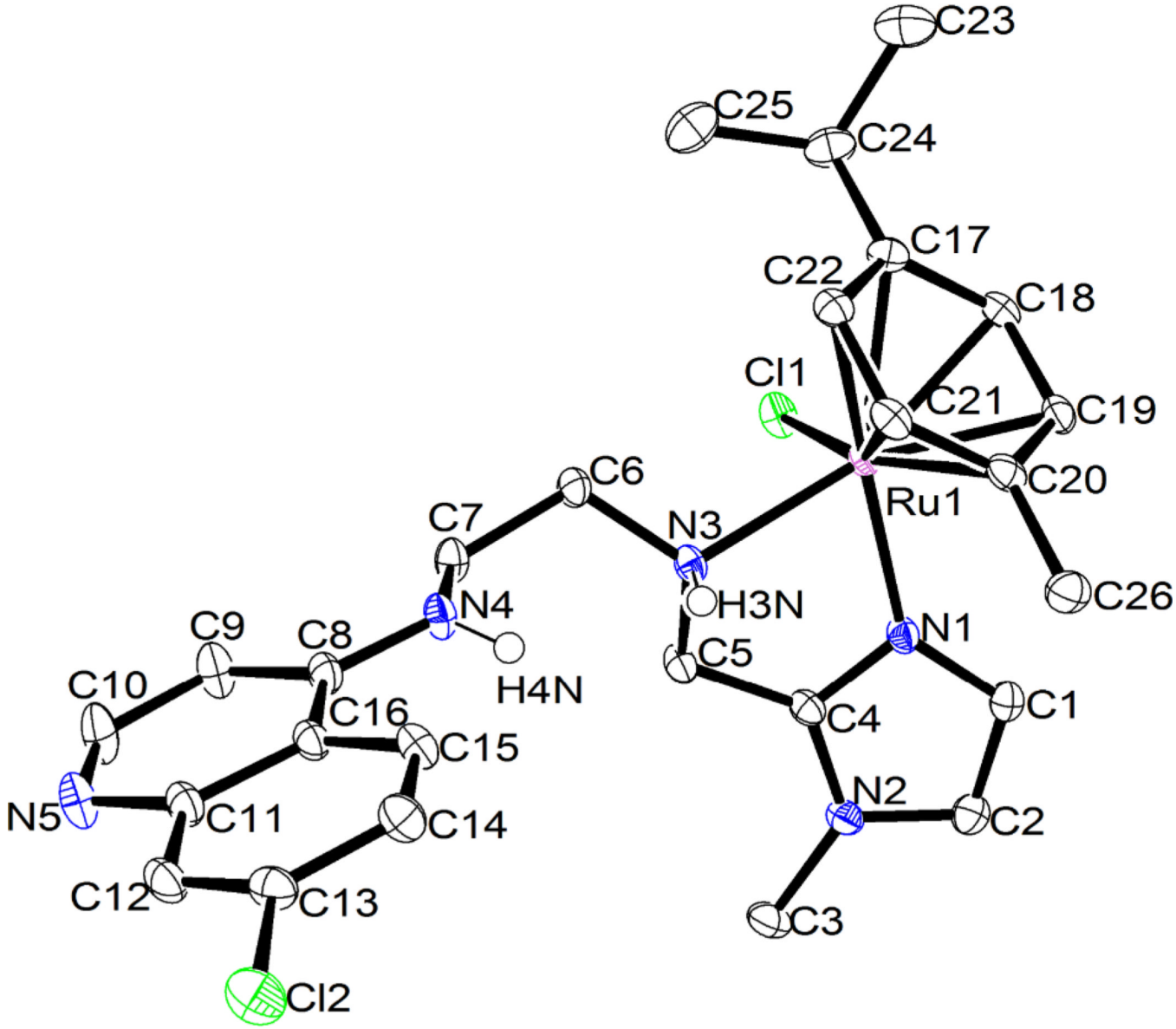

Figure 3.

ORTEP drawing of the molecular structure of **2**·$(CH_3)_2CO$, showing the atom numbering scheme. Thermal ellipsoids are drawn at the 50 % probability level. Solvent of crystallization, the counter ion (Cl^-) and all hydrogens except those of the secondary amines (N3 and N4) have been omitted for clarity (cf. ESI). The ruthenium centre has the R_{Ru} configuration, according to the ligand priority sequence η^6-arene > Cl > $N_{imidazole}$ > N_{amine}, and the chiral aminic nitrogen shows a S_N configuration. Relevant bond lengths (Å) and angles (°): Ru-N(1) 2.078(1); Ru-N(3) 2.169(1); Ru-Cl(1) 2.422(3); Ru-arene centroid 1.66; N(1)-Ru-N(3) 76.47(5); N(1)-Ru-Cl(1) 87.07(3); N(3)-Ru-Cl(1) 85.31(3).

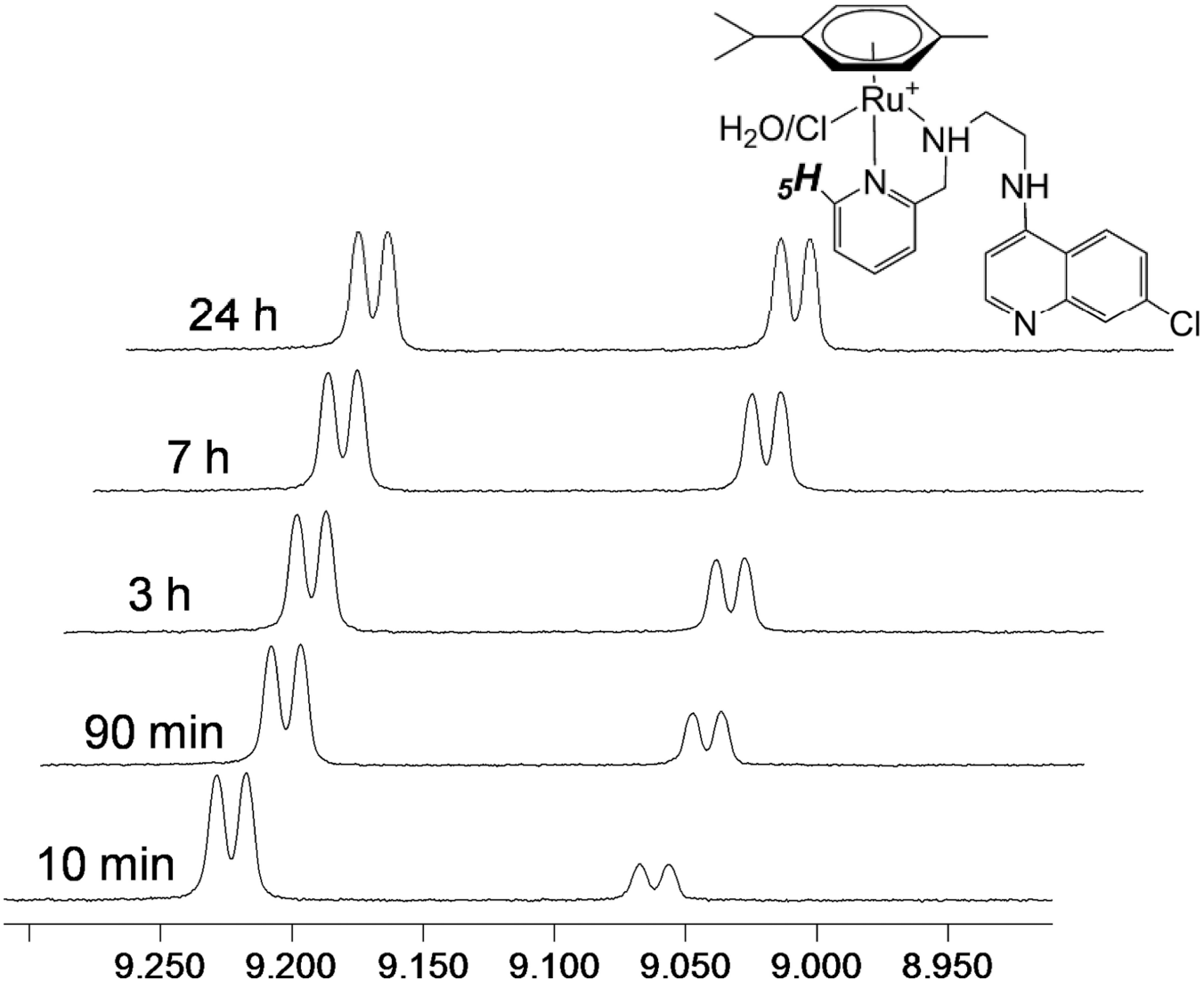

Figure 4.
H5 region of the ^{1}H NMR spectrum of complex **1** at 10 min, 90 min, 3 h, 7 h and 24 h after dissolution in d_6-DMSO.

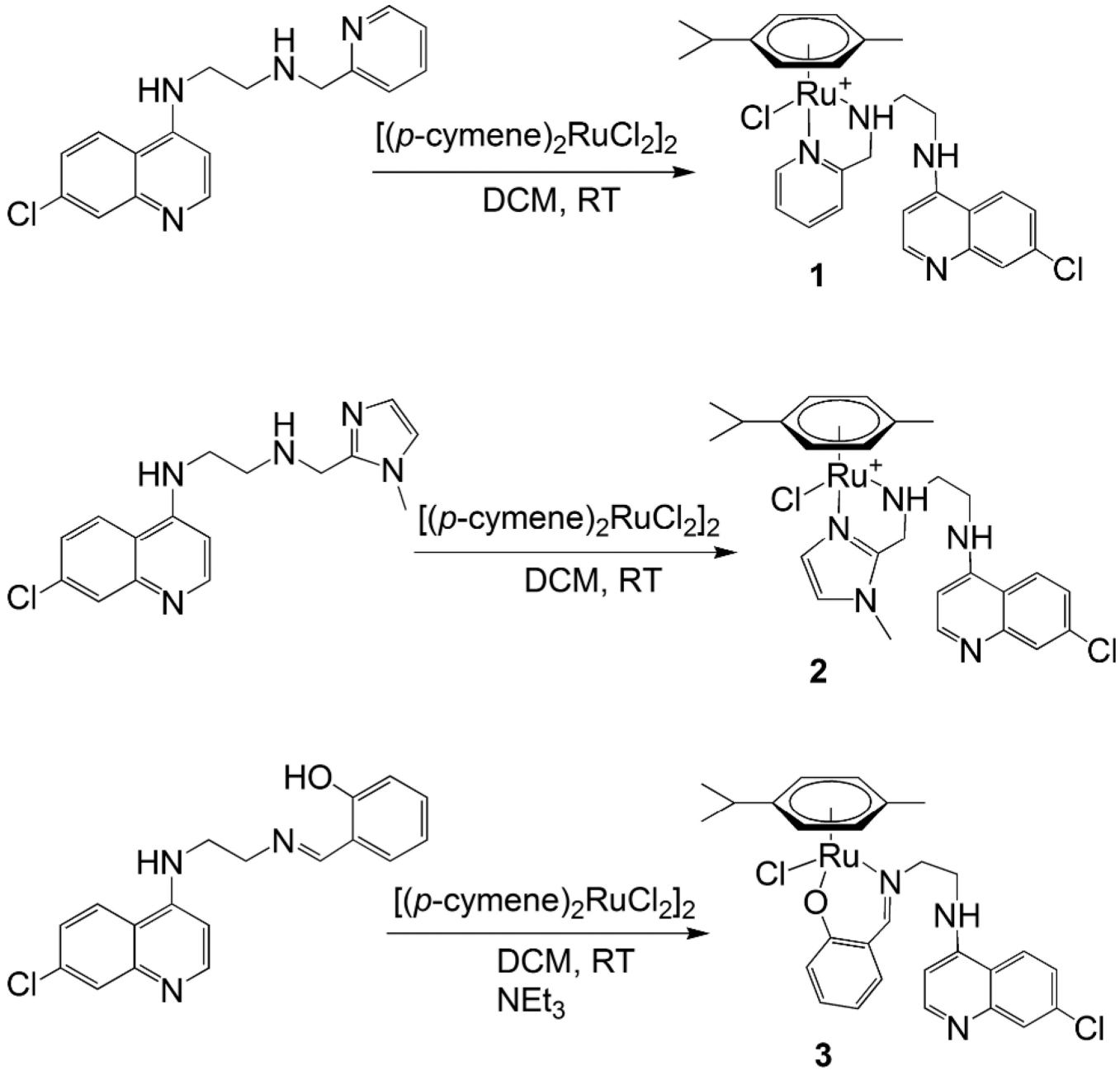

Scheme 1.
Synthesis of complexes **1–3**.

Table 1

Crystal data for **2**·$(CH_3)_2CO$.

	2
empirical formula	$C_{29}H_{38}Cl_3N_5ORu$
fw	680.06
temp (K)	100(2)
λ(Å)	0.71073
cryst syst	Triclinic
space group	P $\bar{1}$
a (Å)	11.3740(4)
b (Å)	12.0484(4)
c (Å)	12.0484(4)
α (deg)	99.6620(10)
β (deg)	106.562(2)
γ (deg)	114.2640(10)
V (Å^3)	1511.68(12)
Z	2
ρ_{calc} (Mg/m^3)	1.494
μ(Mo Kα) (mm^{-1})	0.815
No. reflns.	33271
Unique reflns.	10277
GOOF (F^2)	1.023
R_{int}	0.0260
R1[a] ($I \geq 2\sigma$)	0.0277
wR2[b] ($I \geq 2\sigma$)	0.0609

[a] $R1 = \Sigma||F_O| - |F_C||/\Sigma|F_O|$.

[b] $wR2 = [\Sigma[w(F_O^2 - F_C^2)^2]/\Sigma[w(F_O^2)^2]]^{1/2}$.

Table 2

IC_{50}-values of $\mathbf{L^1}$–$\mathbf{L^4}$ and **1–3** tested *in vitro* for antiplasmodial activity against chloroquine sensitive (D10) and chloroquine resistant (Dd2) strains of *P. falciparum* and for cytotoxicity on Chinese Hamster Ovarian (CHO) cells.

Compound	D10: IC_{50} (μM)	Dd2: IC_{50} (μM)	CHO: IC_{50} (μM)	RI[a]	SI[b]
$\mathbf{L^1}$	0.03 ± 0.002	0.22 ± 0.03	144 ± 50	7.3	4800
$\mathbf{L^2}$	0.19 ± 0.03	0.25 ± 0.06	240 ± 65	1.3	1263
$\mathbf{L^3}$	0.55 ± 0.30	>30	>300	ND	ND
$\mathbf{L^4}$	1.3 ± 0.1	1.3± 0.1	>240	1.0	ND
1	7.69 ± 0.07	21.9 ± 1.0	>160	2.8	ND
2	4.53 ± 0.69	19.7 ± 0.4	>160	4.3	ND
3	0.07 ± 0.007	1.3 ± 0.1	89 ± 19	18.6	1271
CQ	0.025 ± 0.009 (*n* = 7)	0.143 ± 0.014 (*n* = 3)	–		
Emetine	-	-	0.25 ± 0.03 (*n* = 2)		

ND = not determined, *n* = number of data sets averaged

[a] RI (Resistance Index) = IC_{50} Dd2/ IC_{50} D10

[b] SI (Selectivity Index) = IC_{50} CHO/IC_{50} D10

Table 3

Results for heme aggregation inhibition at an acetate buffer (pH=4.9)/n-octanol interface ($HAIR_{50}$) and water/n-octanol distribution coefficient (D) measurements.

Compound	$HAIR_{50}$[a]	D(pH=4.9)[b]	D(pH=6.6)
L[1]	0.95	0.15 ± 0.01	4.24 ± 0.27
1	1.00	0.28 ± 0.04	8.84 ± 0.82
L[2]	1.05	1.68 ± 0.09	2.82 ± 0.16
2	0.86	0.007 ± 0.002	2.06 ± 0.78
L[3]	3.45	0.35 ± 0.02	5.91 ± 0.48
3	1.20	0.40 ± 0.02	1.99 ± 0.10
L[4]	0.87	3.41 ± 0.62	4.39 ± 0.54
CQ[c]	2.92	0.15 ± 0.01	6.61 ± 0.64

[a] $HAIR_{50}$ is the drug to hemin ratio required to inhibit 50% of heme aggregation in comparison to a control experiment with no drug.

[b] D(pH) = [compound] in n-octanol/[compound] in water at the given pH.

[c] As reported in ref.41